40th AIAA/ASME/SAE/ASEE Joint Propulsion Conference & Exhibit
11-14 July, 2004, Fort Lauderdale, Florida

AIAA 2004-3959

Performance Characterization and Vibration Testing of 30-cm Carbon-Carbon Ion Optics

DRAFT – ***Content final but still working on wording, formatting, and style***

John Steven Snyder* and John R. Brophy†
Jet Propulsion Laboratory, California Institute of Technology, Pasadena, CA, 91109

Carbon-based ion optics have the potential to significantly increase the operable life and power ranges of ion thrusters because of reduced erosion rates compared to molybdenum optics. The development of 15-cm and larger diameter grids has encountered many problems, however, not the least of which is the ability to pass vibration testing. JPL has recently developed a new generation of 30-cm carbon-carbon ion optics in order to address these problems and demonstrate the viability of the technology. Perveance, electron backstreaming, and screen grid transparency data are presented for two sets of optics. Vibration testing was successfully performed on two different sets of ion optics with no damage and the results of those tests are compared to models of grid vibrational behavior. It will be shown that the vibration model is a conservative predictor of grid response and can accurately describe test results. There was no change in grid alignment as a result of vibration testing and a slight improvement, if any change at all, in optics performance.

I. Introduction

Carbon-carbon grid technology for ion thrusters has been under investigation for over a decade, and has been recently used in flight applications [D]. Carbon-based materials in general are attractive for ion thruster optics because of their low sputter yields compared to molybdenum, which has been used on the majority of flight thrusters. The use of materials which are more resistant to erosion can directly extend the service life of a thruster [C], or alternatively could permit higher-power operation for a similar service life as present molybdenum designs. Indeed, carbon-based optics are a required technology for aggressive missions such as the proposed Jupiter Icy Moons Orbiter (JIMO) where the xenon throughput requirement of the NEXIS engine is in excess of 2000 kg [G].

Although 10-cm carbon-based ion optics have passed qualification testing [E] and been flown, the design, manufacturing, and testing of larger-diameter grids has been faced with many problems [F]. These include poor dimensional control and other manufacturing issues [REFS], poor voltage standoff [REF], and undesirable grid-to-grid contact [REF] or even breaking during vibration testing. In order to address these problems, the Jet Propulsion Laboratory and Boeing Electron Dynamic Devices, Inc. (EDD) have been working on the Carbon-Based Ion Optics (CBIO) program to develop 30-cm grid technology. The program aims to address critical issues with carbon-based grid technology and bring it to a technology readiness level at which a qualification program may be initiated. Boeing EDD has developed pyrolytic graphite optics (discussed in a companion paper [REF]) while JPL has concentrated on carbon-carbon materials.

Requirements for the CBIO program were developed from the 40-cm NASA Evolutionary Xenon Thruster [REF] (NEXT) program. The CBIO grids are required to meet the performance specifications shown in Table 1, must demonstrate the ability to survive launch-induced vibrational loads and the ability to meet performance specifications afterward, and must demonstrate reduced erosion rates relative to molybdenum. Earlier work in the CBIO program included design and structural modeling of the ion optics assembly, preliminary vibration testing, and voltage standoff testing [A]. The present paper will discuss the production of the carbon-carbon grids and present the results of ion optics performance testing and vibration testing.

---

* Member of the Technical Staff, Advanced Propulsion Technology Group, Member AIAA.
† Section Staff, Thermal and Propulsion Engineering Section, Member AIAA.

Copyright © 2004 by the American Institute of Aeronautics and Astronautics, Inc. The U.S. Government has a royalty-free license to exercise all rights under the copy-right claimed herein for Governmental purposes. All other rights are reserved by the copyright owner.

Table 1. CBIO Grid Performance Requirements.

Operating Point	Beam Current J_B (A)	Beam Voltage V_B (V)	Screen Grid Transparency	Margins	
				Perveance (V)	Electron Back-streaming (V)
TH 1	1.76	1800	0.75	500	100
TH 2	1.76	1400	0.60	100	100
TH 3	1.01	1800	0.75	700	100
TH 4	1.01	1200	0.60	100	100
TH 5	0.75	1800	0.75	800	100
TH 6	0.75	1100	0.60	100	100
TH 7	0.34	1800	0.75	1200	100
TH 8	0.34	679	0.60	100	100

II. Grid Manufacturing

The structural and optical design of the carbon-carbon grids have been discussed elsewhere [A]. Eight complete sets of grids were fabricated in two batches. Four of the grid sets were designed to have NSTAR-like grid thickness and hole patters, the remaining four sets had two different hole patterns, each designed specifically for operation at an Isp of 4000 sec.

Lessons learned from previous carbon-carbon grid manufacturing efforts conducted by JPL were implemented in the CBIO program. Just prior to initiation of the CBIO program a batch of four 30-cm carbon-carbon grids was produced (hereafter referred to as the "pre-CBIO" grids) using the same materials and processes as used in the CBIO grids. New processes implemented in the manufacturing of the pre-CBIO grids vastly improved the control of the grid radius of curvature and sphericity over previous generations of grids, although slight differences in the radius of curvature of the screen and accelerator grids were observed after the heat treatment processing [A]. Although this effect was accounted for in the design of the CBIO tooling, the CBIO grids were also processed in their own individual tooling unlike the pre-CBIO grids which were processed in the same set of tooling. Inspection of the CBIO grids after manufacturing showed that the radius of curvature of both grids changed by approximately the same amount during the processing. As a result, the completed grids have a slightly different radius of curvature which causes a non-uniform grid gap across the span of the optics assembly. Assembly of the optics with uniform grid gap was also hampered by mounting surfaces that, although they included stiffening rings intended to maintain flatness, were not perfectly flat. Sphericity of the grids, as for the pre-CBIO grids, was excellent.

The two largest problems during manufacturing, however, were aperture machining and screen grid fragility. The screen grids were particularly problematic because of the optics performance demands for very thin (350-460 μm), high open-area-fraction (67-70%) surfaces. Of the eight screen grids ordered, one suffered catastrophic damage during handling before delivery, four were delivered to JPL with broken webbings (some only visible under magnification) and/or small areas of delamination but were operable, and one was delivered with heavy soot formation on the downstream surface caused by process-control problems during the carbon-vapor deposition processing. Only two of the screen grids were delivered in good condition. In contrast, all eight of the accelerator grids were delivered in acceptable condition with no broken webbings, delaminations, or other surface imperfections. These results clearly suggest that the manufacturing and process control is mature for the relatively thick, low open-area-fraction grids while improvements are necessary to produce the very thin, high-open-area fraction grids repeatably.

Aperture machining problems were caused less by process control issues than by the transition to a new vendor used for laser machining. The pre-CBIO grids were laser machined by a vendor that could only drill holes parallel to the grid centerline; for CBIO it was desired to machine apertures normal to the grid surface as would be done for a flight-like grid set. Transition to a new vendor that could perform the required work entailed the design of an algorithm that produced the coordinates necessary to drive the 5-axis laser machine tool. Development of the algorithm was complicated by the different radii of curvature in the manufactured grids. Errors were discovered after machining of the first batch which left the grids operational but with the apertures on two of the grid sets

DRAFT

slightly misaligned. This was corrected for the second batch of grids, although other errors in the algorithm and some process control issues produced grids with hole patterns different than the design drawings to varying degrees.

Table 2. CBIO Grid Aperture Measurements.

Grid	Open Area Fraction			Hole Diameter (mm)		
	Design	Actual	Difference	Design	Actual	Difference
Screen 101A	0.668	0.656	-1.8%	1.905	1.880	-1.3%
Accel 101B	0.239	0.216	-9.6%	1.143	1.087	-4.9%
Screen 103A	0.670	0.533	-20.4%	2.300	2.091	-9.1%
Accel 103A	0.239	0.162	-32.2%	1.377	1.156	-16.0%

Specified and as-received hole patterns are shown in Table 2 for two of the grid sets that were tested. Screen grid 101A and accelerator grid 101B were two of the better grids, while grid set 103A was one of the poorest. As will be shown, the poor aperture machining of these grids limited their ability to pass all of the optics performance requirements shown in Table 1.

Although the aperture machining problems and respective corrective actions have been identified, testing of the CBIO grids had to proceed with the as-manufactured grid sets. In general, much new knowledge has been gained during the manufacturing of the CBIO grids and improvement have been made over previous generations of grids, but there are a few remaining manufacturing and process control issues that need to be addressed for future grid productions.

III. Performance Testing

Ion optics performance testing was conducted on the NKO2 thruster (NSTAR-Knock-Off #2) designed and built at JPL to be functionally equivalent to the NSTAR 30-cm ion thruster. The discharge chamber magnetic field, thruster performance, and beamlet current density were all directly measured and found to be essentially the same as for an NSTAR thruster. Tests were performed in a 5.8-m long, 2.4-m diameter cryopumped vacuum facility with base pressure less than 10^{-7} Torr. Thruster mass flow rates were determined from the NSTAR engine throttle table [H] at the equivalent beam current. The discharge current was then adjusted to provide the desired beam current.

A. Performance Measurements

Perveance, electron backstreaming, and screen grid transparency measurements were made over the CBIO throttle table range shown in Table 1. Perveance measurements were made by holding the beam current constant while varying the screen grid voltage and recording the accelerator grid current. The discharge current was adjusted in this case to maintain constant beam current. The perveance limit was defined as the point at which the rate-of-change of current was 0.02 mA/V. Electron backstreaming (EBS) onset was determined by lowering the accelerator grid voltage at constant discharge current and monitoring the beam ion energy cost, a 1% change in which defined the EBS limit. Finally, the screen grid transparency to ions was measured by biasing the screen grid negative of the cathode by twenty volts and recording the bias current. The ratio of the screen power supply current to the total screen current (i.e. bias current plus screen supply current) yielded the transparency. In addition to the optics performance measurements, beam current density profiles were recorded with a standard Faraday probe. Also of interest for carbon-carbon ion optics is the arc rate of the grids during testing. This was monitored during each test using the recycle circuit and a pulse counter in the data acquisition system.

Four separate sets of ion optics were performance tested as a part of the program. As might be expected, those with hole patterns closest to the design drawings had better performance than the others. Performance results for the optics set 101A/B, the set manufactured closest to the design drawings, will be discussed in detail here.

Perveance data acquired with the nominal accelerator grid voltage (V_a) of -200 V are shown in Fig. 1. The baseline accelerator grid current for the highest power is relatively large because of insufficient pumping speed in the test facility. Signs of some crossover impingement are seen in the curve for a 0.34 A beam current at higher

DRAFT

beam voltages. These curves are typical of perveance data acquired with the other optics although there are some differences because of the different geometries.

Electron backstreaming data are shown in Fig. 2 for grid set 101A/B, acquired at a screen grid voltage (V_s) of 1800 V. A sharp drop in beam ion energy cost with accelerator grid voltage was seen for the highest power and more gradual changes for the other operating conditions. The data show that the optics were operated with plenty of EBS margin.

Perveance and EBS limits determined from the data of Figs. 1 and 2 are listed in Table 3 along with the measured screen grid transparencies. Even though the grids did not have the designed hole patterns, they met nearly all of the performance requirements. All of the EBS requirements were met, and all transparency requirements except for the highest power (TH1) were met. The perveance requirements were met for TH3-8 at the nominal accelerator grid voltage of -200 V. When the magnitude of the voltage was increased to -400 V the perveance margin requirements were met and exceeded by 90 V.

The other optics did not meet as many of the requirements as did 101A/B. Grid set 103A, for example, could not even be operated at the TH1 and TH2 levels without excessively high discharge powers because of the low screen grid transparency. That particular grid set met none of the transparency or perveance requirements but it did meet the EBS requirements for TH3-8.

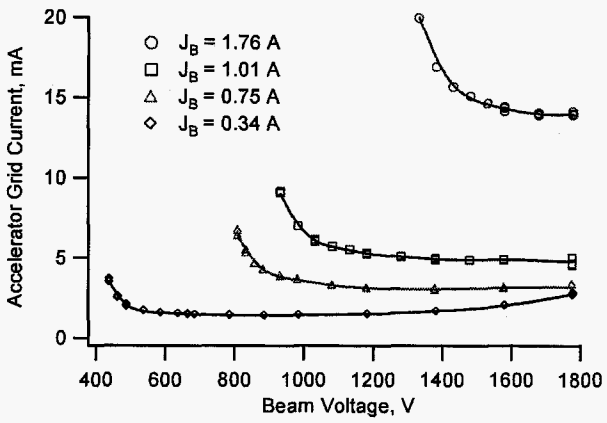

Figure 1. Perveance Data for Grid Set 101A/B at V_a = -200 V.

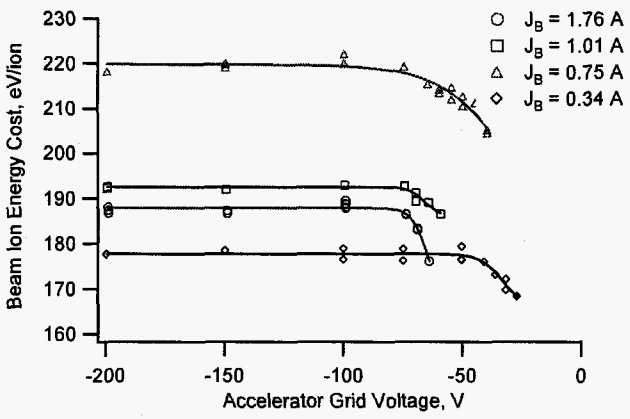

Figure 2. Electron Backstreaming Data for Grid Set 101A/B at V_s = +1800 V.

The ion optics designs were derived from calculations performed with JPL's 2D and 3D ions optics codes. The test results from grid set 101A/B were used as a check against the 2D code results for screen grid transparency. First, the code was used to calculate the transparency for for operating points TH1 (1800 V and 1.76 A) and TH5 (1800 V and 0.75 A). The screen grid transparency is a relatively simple parameter to calculate and the code accurately reproduced the measured results. At TH1 the code predicted a transparency of 0.683, whereas the measurement was 0.682. At TH5 the prediction was 0.773 and the measurement was 0.776. Next, the code was used to calculate the screen grid transparency at TH1 that would have been found if both grids had been produced to the design drawings. The result was a transparency of 0.757, with which it may be stated with some confidence that a properly-machined optics set would have met the requirement. It is more difficult to obtain the perveance limit directly from the codes, on the other hand, so a similar comparison was not made for that parameter.

DRAFT

Table 3. Summary of Optics Performance Measurements for Optics Set 101A/B.

Ion Optics Operating Point			Screen Grid Transparency		Perveance Limit (V)			Electron Backstreaming Limit (V)		
Throttle Level	Beam Current (A)	Beam Voltage (V)	Reqt.	Actual	Measured Limit	Margin Reqt.	Actual Margin	Measured Limit	Margin Reqt.	Actual Margin
TH 1	1.76	1800	0.75	0.681	1435	500	365	70	100	130
TH 2	1.76	1400	0.60	0.630	1435	100	-35	50	100	150
TH 3	1.01	1800	0.75	0.751	1011	700	789	70	100	130
TH 4	1.01	1200	0.60	0.680	1011	100	189	40	100	160
TH 5	0.75	1800	0.75	0.776	863	800	937	65	100	135
TH 6	0.75	1100	0.60	0.695	863	100	237	35	100	165
TH 7	0.34	1800	0.75	0.823	480	1200	1320	35	100	165
TH 8	0.34	679	0.60	0.702	480	100	199	20	100	180

B. Recycle Rate

As discussed in the introduction, the grid-to-grid arc rate has been a source of concern for carbon-carbon ion optics because of the potential for irreparable damage to the grids caused by heavy arcing [B], but a high arc rate alone is not sufficient to cause grid damage. It has been shown that if the total coulomb transfer during an arc event is limited to less than 2.5 mC then the surface damage will not be detrimental to the overall health of the grids [A].

The data acquisition system in the CBIO testing recorded the total number of optics recycles, but many of those recycle events were caused by operating the grids at or near the perveance and electron backstreaming limits. Hence, these should not be considered when determining the grid arc rate.

Recycle data are shown in Fig. 3 for grid set 101A/B, along with total voltage and beam current data for reference. Note that during seven hours of testing, 77 out of 110 recycles occurred at the highest beam current level of 1.76 A during three brief periods of EBS and perveance limit testing. These were caused by operation of the beam power supply too close to its current limit of 2 A. During the first period of operation of the grid set at 1 A of beam current the recycle rate was about 10/hr and this fell to approximately 1.5/hr for the final four hours of testing.

The recycle rate trends in Fig. 3 were typical of those seen for the other optics testing. The recycle rate fell after the first hour or two of testing and, discarding the recycles caused by performance testing, approached some steady value. Grid set 104A reached 4.8/hr at the end of 3 hours of testing and set 104B reached 2.8/hr at the completion of 10 hours of testing. The recycle rate for grid set 103A was much higher than for the other grids (17/hr), but this particular grid set also had a an excessive intragrid electric field stress at the outer edge of the grids. Because of the different radii of curvature of the screen and accelerator grids, the intragrid field was 3.2 kV/mm.

Although these short-duration results are promising, ultimately some long-duration testing in combination with power supplies and equipment designed to meet the 2.5-mC charge transfer specification will be necessary to demonstrate that grid damage caused by arcing will not be an issue for carbon-carbon grids

IV. Vibration Testing

A deliberate, methodical approach of combined modeling and test was implemented in order to develop an understanding of how the optics assembly behaves during vibration testing. Concern was justified by the failure during vibration testing of all known large carbon-carbon grid assemblies (i.e. greater than 10 mm diameter) prior to this work.

The starting point of the vibration modeling is the material properties of the carbon fibers used in the optics assembly. The properties of the laminate structure are calculated using micromechanics models with known

DRAFT

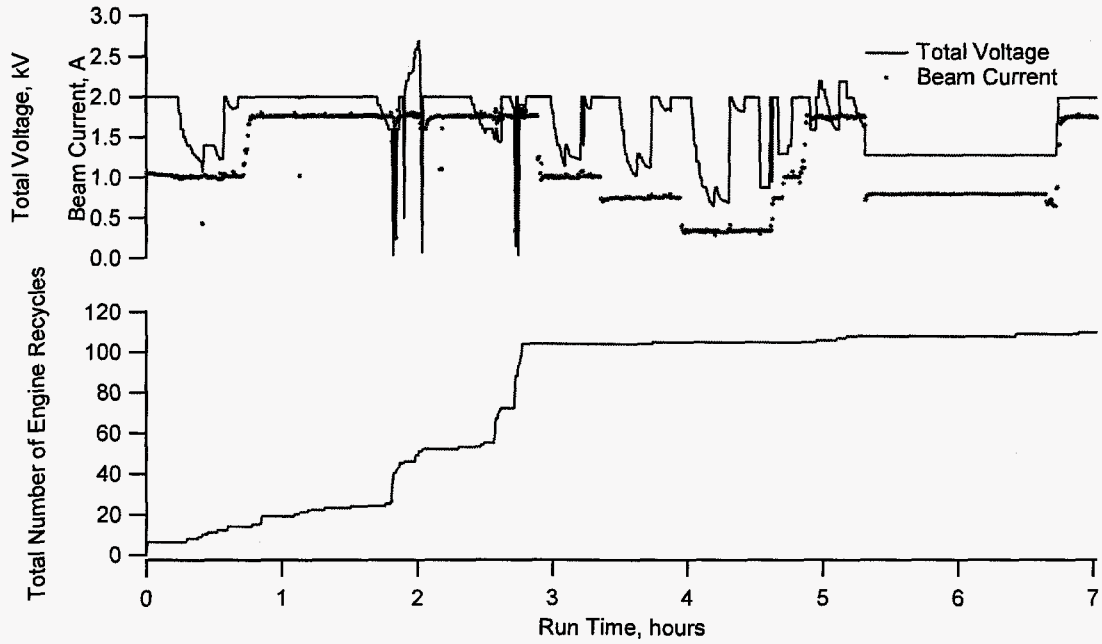

Figure 3. Engine Recycle Behavior During Optics Performance Testing of Grid Set 101A/B.

composite layups and volume fractions. The effective material properties of the active area of the grids are then calculated using the hole pattern and Representative Volume Elements (RVE's) in a finite element model. At this point, a model of the complete optics assembly is built, including the fasteners and isolators used in the assembly. The model is three-dimensional and does not assume symmetry so that all non-symmetric mode shapes are captured. Natural frequencies of the structure may then be determined. A final input to the model is a set of modal damping ratios, which describe the frequency-dependant vibrational damping caused by internal friction in the assembly (e.g. within the laminates, bond joints, and fastener assemblies).

An input vibration spectrum is applied to the assembly at the grid mounting locations for the analysis. Peak stresses are determined by multiplying the RMS levels by a factor of 4.25, which reflects the peaks expected in a narrow-band random process. These stresses are then compared to the calculated material properties. The probability of grid-to-grid contact, the avoidance of which is the main driver for the assembly structural design, is calculated from the RMS displacements of each grid assuming a Gaussian response and Rayleigh narrow-band process distribution of peaks. The probability is quantified as a "safe" grid gap for a 99.99% confidence that there will be no striking during a sixty second test.

Model results are compared to test data through the assembly natural frequencies and total grid response (in Grms). The grid modeling software also produces power spectral density (PSD) curves at arbitrary grid locations which can be directly compared to accelerometer test data. Post-test data analysis is performed by comparing the accelerometer PSD results to test data and adjusting the modal damping ratios until a best fit is achieved (the natural frequencies are independent of damping ratios).

A. Preliminary Testing and Model Development

The grid dynamic models were first validated against test data from vibration of the pre-CBIO optics. As reported earlier [A], very good correlation was achieved between test data and model results for vibration of the accelerator grid alone, typically within a few percent for both natural frequencies and total grid response. It was more difficult, however, to model the screen grid assembly. In general, the correlation between test data and model results was better than ±10% for natural frequency, which is a typical result for carbon-carbon structures modeled with these methods. For total grid response, however, the correlation was only within ±40%, despite best efforts to

DRAFT

adjust the modal damping ratios. This was likely a result of the increased complexity of the carbon-carbon structure compared to the accelerator grid.

Because of the success in modeling the accelerator grid in comparison to the more complex screen grid assembly, it was reasoned that the fundamental methods and materials properties used in the model were sufficiently accurate and it was recognized that those properties which are difficult or impossible to model with precision would limit the ultimate accuracy of the vibration model.

The results obtained by model correlation with independent grid tests were next used to predict the behavior of the optics assembly. In addition to the screen and accelerator grid assemblies, the full optics assembly included the twelve isolator stacks, comprised of isolating standoffs, bolts, washers, and shims. The pre-test modeling predicted that at the NSTAR AT vibration level of 9.1 Grms there would be no grid overstress conditions and that the grids would not strike each other, although at the QT level of 12.7 Grms there was only an 85% confidence level of no striking during a sixty second test.

The grids were successfully vibrated at the NSTAR AT level of 9.1 Grms for 60 seconds, with no damage to either grid and no grid-to-grid contact. Subsequent to that test, the grids were vibrated at 12.7 Grms for a duration of only thirteen seconds, again with no damage to either grid and no grid-to-grid contact.

Modeling and test results are shown in Table 4 for accelerometers that were mounted on the active area of the accelerator grid. Accelerometer measurements were a factor of two to three lower than the pre-test predictions. This is almost certainly due to additional damping in the optics isolator stacks, including the interfaces with the carbon-carbon material, which was not factored into the pre-test modeling. Whereas the pre-test predictions used modal damping of 0.1% for all modes except two which were set to 0.6%, the post-test model had a first-mode damping of 10% and damping of up to 2% for several other modes. Post-test data analysis and modeling achieved correlation with the test data of 10% or better for the accelerator grid data. Correlation of screen grid data with the model was within 30%.

Table 4. Comparison of pre-CBIO Vibration Test Data and Model Calculations for Accelerator Grid.

Location		Pre-test Calculation (Grms)	Vibe Test Measurement (Grms)	Post-test Calculation (Grms)	Difference Between Test and Post-Test Calculation
Radius (cm)	Angle (deg)				
0.0	0	244.4	84.1	80.6	-4%
2.1	90	123.0	70.7	62.5	-10%
6.4	180	211.4	75.8	68.5	-10%
10.2	180	229.1	107.7	115.5	+7%

Vibration testing of the pre-CBIO grids proved for the first time that larger-diameter carbon-carbon ion optics, when properly designed, can survive launch-induced vibrational loads with no damage. The modeling results showed that (1) the materials properties and modeling methods used are appropriate for these carbon-carbon grids, and (2) unfortunately, the ultimate structural response of the full optics assembly is dominated by damping in the structural interfaces which is difficult to accurately predict and model. The use of conservative damping ratios, however, yields a good conservative model of grid vibrational response.

B. Vibration Testing of CBIO Grids

One major goal of the CBIO program is to demonstrate not only that carbon-carbon grids can survive vibration testing, but that they can do so with no change in optics performance. To that end, a single optics set was chosen to undergo combined performance and vibration testing. In addition, vibration testing was to be performed on an NSTAR engineering model thruster, in this case EMT1c which has been used for other vibration testing [REF Haag's PG paper].

DRAFT

1. Preliminary Activities

CBIO grid set #103A was selected for the combined performance/vibration testing, largely because the screen grid was in the best physical condition. Although the hole pattern of the optics was significantly different than the design (as shown in Table 2), it will be shown that this has little effect on the overall structural response of the grid set.

Visual inspection of the grids before assembly showed some minor surface features (e.g. light surface scratching, imperfect bond joints) but no cracks, delaminations, broken webbings, or missing plies. The optics set was assembled with twelve fastener stacks, each of which included exactly two shims sized to achieve the proper grid gap. All bolts were torqued to 25 in-lbs. A breakdown of the optics set mass is given in Table 5. The grid gap at the optics centerline was measured to be 0.855 ± 0.023 mm and the gap at the periphery was 0.620 ± 0.025 mm.

Table 5. Mass Breakdown of Optics Assembly 103A.

	Mass (gm)	Qty.	Total (gm)
Accelerator Grid Assembly	321.0	1	321.0
Screen Grid Assembly	513.7	1	513.7
Fastener Stack (nominal)	29.7	12	356.4
		Total Assembly Mass:	1.19 kg

The grids were aligned visually and then the center and six surrounding apertures were inspected for to determine the optics alignment. For each hole on the screen and accelerator grids, the location of the hole center in Cartesian coordinates was determined to within ± 0.01 mm. From these results, the average distance between the centerlines of the screen and accelerator apertures was determined to be 0.034 ± 0.012 mm. After these pre-test characterizations, the optics went through performance testing (the results are shown later in this section).

A preliminary vibration test was performed without the ion optics installed on the thruster in order to obtain the inputs necessary for vibration modeling. Accelerometers were placed on the grid mounts and recorded the response to NSTAR AT-level vibration. Although the levels seen by the optics during the full test are different when their mass and structure is added to the thruster, an estimate of the grid forcing function was necessary. The response of two of the accelerometers is shown along with the input spectrum in Fig. 4. The vibration level at the grid mounting locations was about 18 Grms, roughly twice the input at the vibration table. Pre-test vibration modeling was performed using the response spectra in Fig. 4 and the modal damping ratios determined from pre-CBIO full-optics testing. The model predicted no overstress or overstrain conditions for any portion of the optics assembly and a safe grid gap of 0.53 mm, 40% smaller than the actual grid gap.

2. Vibration Testing and Analysis

For the full vibration test the screen and accelerator grids were instrumented with four accelerometers each and an electrical circuit to detect grid-to-grid contact. The contact circuit consisted of a power supply to create a small voltage difference between the grids, a current-limiting resistor, and an oscilloscope set to trigger on voltage collapse. All accelerometers were adhered to grid surfaces by applying a small portion of Kapton tape to the desired location then bonding the accelerometer to the tape with epoxy. This method was used to avoid epoxy residue on the optics after testing. The accelerometer locations are shown in Table 6, where an arbitrary coordinate system with center at the grid centerline was used. All

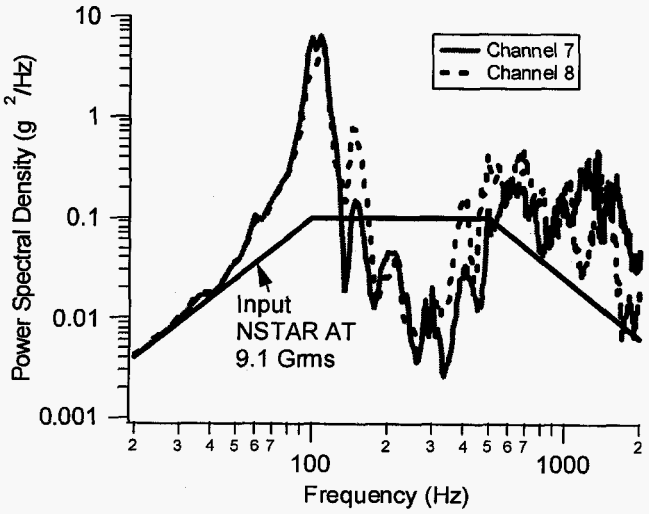

Figure 4. Vibration Response of EMT1c Without Ion Optics.

DRAFT

of the screen grid accelerometers were located on the upstream portion of the grid at the edge of the active area. Although data from the active area of the screen grid was desired, the risk of damage to the fragile grid during accelerometer placement was too great. Accelerometer placement on the accelerator grid was at the centerline, two intermediate points along the span, and at the flat edge of the grid just inside the stiffening ring. One accelerometer was placed on the optics mounting ring of the thruster. A photograph of the test setup is shown in Fig. 5.

Table 6. Accelerometer Placement for Vibration Test.

#	Location	Grid Coordinates	
		Radius (cm)	Angle (deg)
1	Screen Grid	14.7	0
2	Screen Grid	14.7	45
3	Screen Grid	14.7	270
4	Screen Grid	14.7	225
5	Accel Grid	0.0	0
6	Accel Grid	2.1	90
8	Accel Grid	10.2	180
10	Accel Grid	15.9	0

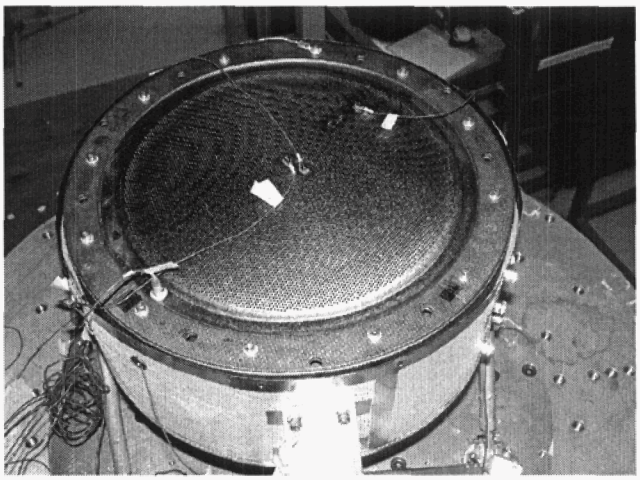

Figure 5. Vibration Test Setup.

After a preliminary sine sweep test, the full random vibration test was performed according to the test schedule in Table 7, where 0 dB is the NSTAR AT vibe level of 9.1 Grms. Accelerometer measurements were taken at the full test level as well as at -12 dB before and after the full-level test. The test was performed without incident and no grid-to-grid contact was detected at any time during the test. Post-test visual inspection showed no damage to either grid. Comparison of the -12 dB data, shown in Fig. 6 for the accelerator grid centerline, showed no hidden damage to the optics.

The responses of the four screen grid accelerometers were similar to each other, as was expected based on the locations and azimuthal symmetry of the optics. The total response on the screen grid ranged from 21 to 26 Grms. The total responses on the accelerator grid were slightly less, ranging from 18 to 22 Grms. Typical data from the accelerometers are shown in Fig. 7.

Table 7. Random Vibration Test Schedule.

Vibration Level	Task	Time (min:sec)	
		Level	Cumulative
-12 dB	Hold	0:30	0:30
-12 dB	Measurement	0:10	0:40
-9 dB	Hold	0:10	0:50
-6 dB	Hold	0:10	1:00
-3 dB	Hold	0:10	1:10
0 dB	Hold	0:50	2:00
0 dB	Measurement	0:10	2:10
-6 dB	Hold	0:10	2:20
-12 dB	Hold	0:30	2:50
-12 dB	Measurement	0:10	3:00

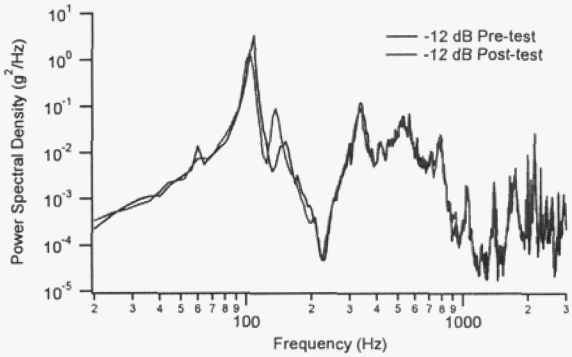

Figure 6. Comparison of -12 dB Measurements on Accel Grid Centerline.

DRAFT

As was done for all previous grid vibration tests, the accelerometer data were analyzed and post-test modeling was performed to determine the most probable modal damping ratios. This analysis was complicated because the input spectrum to the grid assembly could not be directly measured and hence was unknown. Therefore, post-test modeling was performed using the vibration data from the thruster-only test.

The pre-test predictions for total response, as for the pre-CBIO testing, were conservative. The inclusion of shims within the isolator stacks for the 103A assembly (not included in the pre-CBIO stacks) likely introduced additional interface damping. The predicted response on the accelerator grid centerline was 81 Grms, whereas the measured value was 23 Grms. Modal damping ratios determined during the post-test analysis were as high as 42% for the first few modes with nine others set in the range of 10 to 20%, compared with the range of up to 10% found in the pre-CBIO analysis. Post-test calculations of the total responses were within 30% of the test data for all accelerometers.

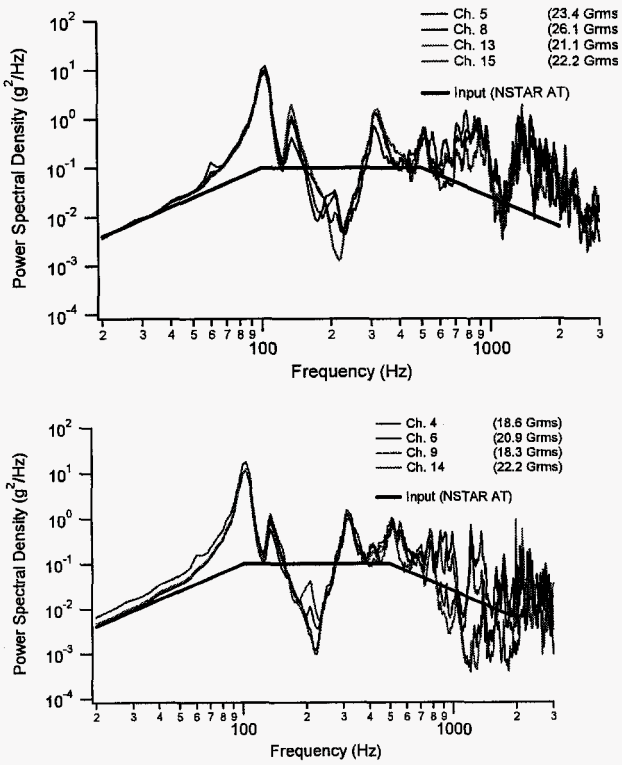

Figure 7. Typical Accelerometer Data from CBIO Vibration Test.

Differences in pre-test predictions and measured data are probably also due to the difference between the real and assumed vibration input to the optics assembly. Because the real vibration input to the grids was unknown and the thruster-only data were assumed to be the input during analysis of the full test, the modal damping ratios calculated after the test must also inherently include the differences between the real and assumed inputs. For this reason, these damping ratios are probably not applicable to tests on other thrusters or to the grids by themselves.

As a final exercise for this portion of the project, a vibration analysis was performed for grid set #103 in the as-designed condition instead of the as-received condition. This was done using the modal damping ratios determined from the post-test data analysis. There was very little difference in the predicted response of the grids, as shown in Table 8, in spite of the significant differences in the optics dimensions. This is yet another indication of the importance of the strong structural design and the large influence of the modal damping.

Table 8. Comparison of Calculated Accelerometer Responses for As-Received and As-Designed CBIO 103A Optics Assembly.

#	As-Received	As-Designed	Difference
1	24.0	22.7	5.4%
2	24.0	22.5	6.3%
3	24.0	22.5	6.3%
4	22.4	21.1	5.8%
5	21.2	20.9	1.4%
6	21.2	20.9	1.4%
8	20.8	20.4	1.9%
10	18.0	18.1	-0.6%

3. Post-Test Optics Characterization and Performance Testing

After completion of the test, the optics gap and alignment were inspected and compared to pre-test measurements. As the results in Table 9 show, there was no measurable change in grid gap or grid alignment. Perveance data acquired before and after the vibration test are shown in Fig. 8. For all three beam currents the accelerator grid currents were slightly lower when measured after the vibration test. The perveance limits also

DRAFT

decreased slightly. All pre- and post-test optics performance measurements are summarized in Table 10. As can be seen, there was little change in performance, with the values of most parameters showing a slight improvement.

Table 9. Pre- and Post-Test Assembly Inspection Results.

	Centerline Grid Gap	Translational Alignment
Before Vibration Test	0.855 ± 0.023 mm	0.034 ± 0.012 mm
After Vibration Test	0.855 ± 0.051 mm	0.030 ± 0.022 mm

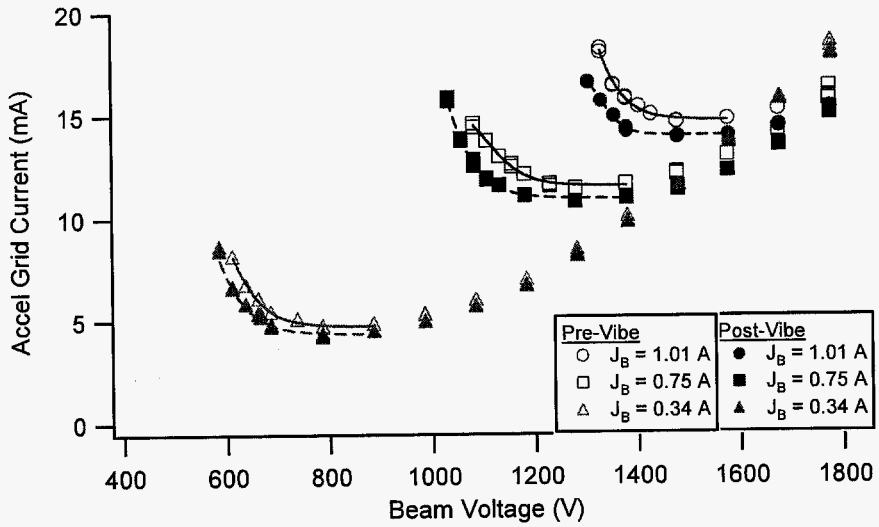

Figure 8. Perveance Data Acquired Before and After Vibration Testing.

Table 10. Summary of Optics Performance Results Before and After Vibration Testing.

Set Points			Screen Grid Transparency			Perveance Limit				EBS Limit		
Operating Point	J_B	V_B	*Pre-Test*	*Post-Test*	*Difference*	*Pre-Test*	*Post-Test*	*Difference (V)*	*Difference (%)*	*Pre-Test*	*Post-Test*	*Difference*
1	1.76	1800										
2	1.76	1400										
3	1.01	1800	59.4%	59.9%	0.5%	1390	1368	-22	-1.6%	60	60	0
4	1.01	1200	0.541 (1400V)	.545 (1400V)	0.4%	1390	1368	-22	-1.6%			
5	0.75	1800	63.2%	63.7%	0.5%	1156	1112	-44	-3.8%	60	55	-5
6	0.75	1100	53.4%	53.8%	0.4%	1156	1112	-44	-3.8%	25	25	0
7	0.34	1800	74.1%	74.3%	0.2%	679	654	-25	-3.7%	25	30	5
8	0.34	679	54.6%	55.7%	1.1%	679	654	-25	-3.7%	15	15	0

V. Conclusion

Eight sets of 30-cm carbon-carbon ion optics were designed and manufactured as a part of the CBIO program and, for the first time, the viability of this technology for flight applications of 30-cm-diameter and larger grids has been proven. Although there were problems during grid production which resulted in imperfect grids, those which were most detrimental to grid operation and performance are understood and corrective actions have been identified. This development was the first attempt to produce 30-cm dished screen grids with thickness less than 500 μm and the low success rate (only two of eight were produced without visible material defects) indicates that the

DRAFT

manufacturing and process controls need to be improved for the very thin, high open-area-fraction grids. The material quality of all eight accelerator grids was excellent.

In spite of the issues with grid production, grid set 101A/B which was designed to have an NSTAR-like hole pattern met all of the performance requirements except for screen grid transparency at the highest power (TH1). Ion optics modeling predicted that a correctly-made grid set would have passed this test. The ability of other grid sets to meet the performance requirements was adversely affected by poor hole machining. The arc rate of all grids was low for newly-manufactured grid sets (i.e. a few per hour); one set had a higher arc rate likely because of excessive intra-grid electric fields over a relatively large area.

Two separate sets of 30-cm dished carbon-carbon grids were successfully vibration tested to NSTAR AT levels (9.1 Grms) without any damage or grid-to-grid contact. For CBIO grid set 103A, the vibration testing was performed on the NSTAR engineering model thruster EMT1c where the vibration loading presented to the grids was much higher than the NSTAR specification. Vibration models were developed and validated in conjunction with this testing. The model can predict natural frequencies to within 15% and can be used to make conservative pre-test predictions of total response and the probably of grid-to-grid contact. The overall grid response is dominated by internal damping, much of which appears to occur in the isolators and fasteners used to assemble the grid set, and which is difficult to predict for any given test configuration. Post-test analysis produces results which correspond to test data to within 30-40% and can be used to examine the effects of small changes in grid design. There was no measurable change in the grid gap or grid alignment of grid set 103A as a result of vibration testing. In addition, there was little-to-no change in the optics performance as a result of vibration testing.

The performance and vibration testing described herein have demonstrated the viability of carbon-carbon grid technology for 30-cm and larger ion thrusters. In March, 2004, a 2000-hour endurance test was initiated in order to demonstrate the expected erosion rates relative to molybdenum on a 30-cm thruster; results of the test will be presented in a forthcoming paper. With the combined results of these works, carbon-carbon ion optics can be baselined on proposed missions such as JIMO with confidence.

Acknowledgments

The authors would like to acknowledge the large contributions of Dr. Brian Sullivan and the team at Materials Research & Design, Inc., for the vibration modeling and analysis. Vibration testing was performed in the vibration lab at Boeing EDD and was successful because of the support of Andrew Hanna and the lab technicians. The NKO2 thruster was built by Mr. Allison Owens and Mr. Ray Swindlehurst of JPL. Thanks to Dr. Wei Shih of Allcomp, Inc., for fabrication of the carbon-carbon grids.

This research was carried out, in part, at the Jet Propulsion Laboratory, California Institute of Technology, under a contract with the National Aeronautics and Space Administration. Funding was provided by the In-Space Transportation Program managed by Jim Robinson at the NASA Marshall Space Flight Center. The CBIO program is managed by Randy Baggett. Their support is gratefully acknowledged.

References

(work in progress....)

[A] JPC03 CBIO, 2003-4716
[B] Japanese paper with bad arcing
[C] Ref 10 of A.
[D] MUSES JPC03?
[E] MUSES qual test
[F]
[G] jay's jpc paper 2003
[H] NSTAR throttle table

DRAFT